Arch. Metall. Mater. **67** (2022), 4, 1427-1434

DOI: https://doi.org/10.24425/amm.2022.141070

NIDA KATI[1*], SERMIN OZAN[1], TÜLAY YILDIZ[1], MEHMET ARSLAN[1]

EFFECT OF REACTION TIME AND HEAT TREATMENT IN THE PRODUCTION OF HYDROXYAPATITE BY HYDROTHERMAL SYNTHESIS

In the present work, Hydroxyapatite synthesis was carried out using hydrothermal method with calcium nitrate tetrahydrate ($Ca(NO_3)_2.4H_2O$) and fosfor pentaoksit (P_2O_5) as precursors. For the hydrothermal method, constant reaction temperature (180°C) and different reaction times (6 hours, 12 hours, 18 hours and 24 hours) were determined. The samples produced were divided into two groups. Four samples were not heat treatment; four samples were heat treatment at 700°C for 1 hour. The obtained products were characterized by scanning electron microscopy (SEM), energy dispersive spectroscopy (EDS) techniques, X-ray diffraction (XRD) and UV-Vis spectrometer. SEM photos showed that the Hydroxyapatite powders produced are in the form of the agglomerate. According to EDS results, Hydroxyapatite samples are of high purity. XRD's findings confirm that the diffraction peaks correspond to the pure phase of Hydroxyapatite. A general decrease was observed in the energy band gap of the samples with increasing hydrothermal reaction time.

Keywords: Hydroxyapatite; Hydrothermal; Heat treatment; Reaction time; XRD/SEM; optical properties

1. Introduction

Hydroxyapatite (HA), a type of the calcium phosphate family, is one of the most common bioceramic materials, and its chemical formula is $Ca_{10}(PO_4)_6(OH)_2$. HA has a hexagonal crystal structure with a = b = 0.942 nm and c = 0.688 nm unit cell dimensions [1]. Due to its excellent biocompatibility, lack of toxicity, bioactivity and strong adsorbent properties, it is commonly used in biomedical and non-biomedical fields in either pure, doped or composite form [2-4].

A broad variety of traditional approaches are present in the literature for the synthesis of HA products including precipitation, hydrothermal, sol-gel, sonochemical, biomimetic, and many more [4,5]. One of the most important of these methods is the hydrothermal synthesis method. In hydrothermal synthesis, synthesis conditions such as reaction time, reaction temperature, solution concentrations and pH values can be changed. Hydrothermal synthesis is a simple and cost effective process to obtain controllable different morphologies due to the use of temperature and pressure in the autoclave chamber [1].

Hydrothermal is a form that requires reorganization of the molecular or ionic structure substance in aqueous solution at high temperatures and pressure in an autoclave or pressure tank. The hydrothermal method is expressed as chemical precipitation where aging occurs at high temperatures and high pressures [2,3].

When the literature on various aspects of HAp nanoparticles was examined, Doremus et al. [4] conducted a study on the processing of bioceramics and their mechanical properties. Orlovskii et al. [5] It was determined that they studied three HAp synthesis methods as chemical precipitation, solid-state synthesis and hydrothermal method. Ferraz et al. [6] and Norton et al. [7] conducted various studies on HAp preparation, especially using wet chemical procedures. Dorozhkin [8], Zhou and Lee [9] examined studies reporting the preparation of HAp and its application to various biomaterials. Sadat-shojai et al. investigated the synthesis methods for nanosized Hydroxyapatite structures with different structures. Critical properties of Hydroxyapatite can be controlled effectively by changing the synthesis parameters [2]. He et al. investigated the effect of hydrothermal process temperature on Hydroxyapatite coatings deposited by the electrochemical method. They stated that at 180°C, the Hydroxyapatite coating reached its maximum crystallinity [10]. Shih et al. investigated the crystal growth and morphology of nano-sized Hydroxyapatite powders synthesized from dicalcium phosphate dihydrate ($CaHPO_4 \cdot 2H_2O$, DCPD) and $CaCO_3$. They stated that the crystallinity of Hydroxyapatite powders increased with the increase in

[1] FIRAT UNIVERSITY, FACULTY OF TECHNOLOGY, METALLURGICAL AND MATERIALS ENGINEERING DEPARTMENT, 23200, ELAZIĞ, TURKIYE

* Corresponding author: nkati@firat.edu.tr

heat treatment temperature and time[11]. Syukkolova et al. conducted a study on the effect of the reaction environment and hydrothermal synthesis conditions on the morphological parameters and thermal behavior of calcium phosphate nanoparticles [12]. Ortiz et al. used two different pH stabilizers that carried out the synthesis of Hydroxyapatite by hydrothermal method. Solution pH parameter is an important parameter that directly affects the final morphology and structure of Hydroxyapatite [13]. Jin et al., colloidal hydrophilic Hydroxyapatite nanorods were synthesized by hydrothermal method in the presence of sodium citrate [14]. Guo et al. synthesized mesoporous carbonate Hydroxyapatite microspheres from calcium carbonate microspheres by hydrothermal method [15]. Daryan et al. HA microspheres with nanostructures on the surface were prepared by hydrothermal method using EDTMP as a regulating agent. They stated that constant pH and EDTMP concentration increasing over time led to a gradual change in surface morphology of microspheres from nanosheets to nanorods [16]. Zhu et al. synthesized Hydroxyapatite $Ca(NO_3)_2{\cdot}4H_2O$ and H_3PO_4 by hydrothermal method. Hydrothermal synthesis of HA produces long columnar crystals. They indicated that pH, reaction temperature, hydrothermal reaction time and calcium ion concentration strongly influenced the microstructure and growth of HA crystals [17]. Negret et al. synthesized Hydroxyapatite nanorods by hydrothermal method that does not surfactant-free. The reaction temperature and reaction time are very effective on particle size. Although there is a good reaction time of 8 hours, they stated that well crystalline nanorods are obtained when the hydrothermal reaction is carried out for 12 hours [18]. Kong et al. synthesized the layered Hydroxyapatite by hydrothermal process using surfactant template. In general, while Hydroxyapatite was spherical or rod-shaped, the Hydroxyapatite synthesized in this study had a layer-by-layer structure, proving that carbonate ions play crucial roles in shaping the LCHA layer during the crystal growth process [19]. Liang et al. stated that the crystallinity, morphology and size of the nanoapatite crystals were significantly affected by the hydrothermal synthesis conditions. They obtained high crystallinity and large crystal sizes at high hydrothermal temperatures and long hydrothermal times [20].

Considering the literature studies, it is seen that there are many studies on the production of Hydroxyapatite by hydrothermal method. In the studies, mostly additives and surfactant were used. This study, it is aimed to produce Hydroxyapatite nanopowders without using additives and surfactant by hydrothermal method under high pressure at constant reaction temperature and at different reaction times. By applying heat treatment to a group of these samples, the effects of heat treatment were also examined. SEM, EDX, XRD and Uv-Vis characterizations of the produced Hydroxyapatite samples were made. There is very little work in the literature on the Uv-Vis characterization of Hydroxyapatite nanopowder. This study will contribute to the literature on the optical properties and energy band gap of Hydroxyapatite nanopowder.

The remaining part of this paper is as follows; section two presents experimental studies, section three briefs experimental results and discussions, section four presents conclusions.

2. Material and methods

2.1. Materials and sample preparation

In this study, pure calcium nitrate tetrahydrate ($Ca(NO_3)_2{\cdot}4H_2O$), commercially available from Sigma-Aldrich, was weighed 2.3615 g on a precision balance and put in a beaker of 40 ml deionized water. Similarly, pure phosphorus Pentoxide (P_2O_5) was measured 0.8517 g and put in a beaker of 40 ml of deionized water. The solutions were mixed separately in the magnetic stirrer for 60 minutes at 500 rpm until dissolution. For the solutions to have a homogeneous structure, they were mixed in the ultrasonic bath for 10 more minutes. The solutions taken from the ultrasonic bath were combined and NH_4OH (Ammonium Hydroxide) was added. After the pH of the solution was raised to 11, it was mixed again in the magnetic stirrer for 60 minutes at 500 rpm. The suspension obtained was transferred to an 80 ml Teflon lined autoclave (100 ml PTFE, Fytronix). Hydroxyapatite powders were produced by the Hydrothermal method at the parameters given in TABLE 1. For the hydrothermal method, constant reaction temperature (180°C), constant reaction pressure (10 bar) and different reaction times (6 hours, 12 hours, 18 hours and 24 hours) were determined. The samples produced are divided into two groups. Four samples were not heat treatment; four samples were heat treatment at 700°C for 1 hour.

TABLE 1

Sample Production Parameters

Production parameters				
Sample	Temperature (°C)	Time (h)	Heat treatment parameters	
			Temperature (°C)	Time (h)
HA-6h	180	6	Non-heat treatment	
HA-12h	180	12		
HA-18h	180	18		
HA-24h	180	24		
HA-6h-HT	180	6	700	1
HA-12h-HT	180	12		
HA-18h-HT	180	18		
HA-24h-HT	180	24		

2.2. Surface characterization

In this study, the surface morphologies and chemical compositions of Hydroxyapatite powders produced by the Hydrothermal method were examined using a ZEISS EVO LS 10 brand field emission scanning electron microscope (SEM) equipped with energy dispersive spectroscopy (EDS). Secondary electrons were used under 15 kV in SEM analysis. XRD analyzes were performed with a Bruker D8 advance anode X-ray diffractometer at $\lambda = 1.5406$ wavelength, 40 kV and 15 mA current, and 2°/min scanning speed. The nanopowders were formed into 4 mm pellets with the help of a desktop hydraulic press for

UV-Vis measurements, and then characterization was performed with a Shimadzu 3600 UV/VIS spectrometer in the wavelength range of 200-600 nm.

3. Results and discussion

3.1. SEM and EDX analysis

SEM analyzes of Hydroxyapatite powders produced by hydrothermal method were performed at 50000× magnifications. Fig. 1 shows the SEM images of HA-6h, HA-12h, HA-18h and HA-24h, while Fig. 2 shows SEM images of HA-6h-HT, HA-12h-HT, HA-18h-HT and HA-24h-HT samples.

In nanopowder production, reaction temperature, reaction time and pH values of the solution used in the reaction are the most effective parameters affecting particle size and morphology. In our study, different synthesis times were studied by keeping the synthesis temperature constant. The characteristic structure of the powders produced by the hydrothermal method is in the form of Hydroxyapatite crystals. It is possible to obtain various morphologies and particle sizes in the hydrothermal method. When SEM images are examined, it is seen that the particles in the synthesized Hydroxyapatite powders are in the form of agglomerates. Agglomeration is an inherent state of nanopowder due to its high energy surface [21,22]. As the sintering time increases, more clumping occurs. Thus, the particle size increases. The aggregation of particles can occur during the drying process due to Ostwald ripening [23].

The formation of Hydroxyapatite crystals occurs in two stages. The first stage is the initiation of nucleation and the second stage is the growth of nucleation. In the first stage, only small Hydroxyapatite crystals are formed, with increasing time small crystallites turn into large prisms. Zhu et al. stated that the crystal growth and crystal dissolution process reached equilibrium after 12 hours in their study. In this process, some of the smaller crystals dissolve simultaneously, the larger ones recrystallize, so some crystals shrink and some crystals grow [24]. Crystal growth in the hydrothermal method is a phase transformation process that takes place in an airtight container, at high temperature, under high pressure limited by aqueous solution. Therefore, the addition of impurity and system temperature greatly affects resolution and recrystallization [25].

EDX analysis results of Hydroxyapatite powders produced by the hydrothermal method are given in Fig. 3 and TABLE 2. EDX analysis was performed on HA-6h, HA-12h and HA-24h-HT samples in order to see the element distribution. It has been observed that the Hydroxyapatite nanoparticles are of high purity. As expected, all EDX samples contain calcium, phosphorus, oxygen and carbon. The presence of Ca, P and O elements indicated the formation of apatite in both nanopowders. In addition, the existence of a carbon element confirmed the carbonated structure of apatite crystals. Thus, the process, molecular and elementary structures were in full agreement with each other [21].

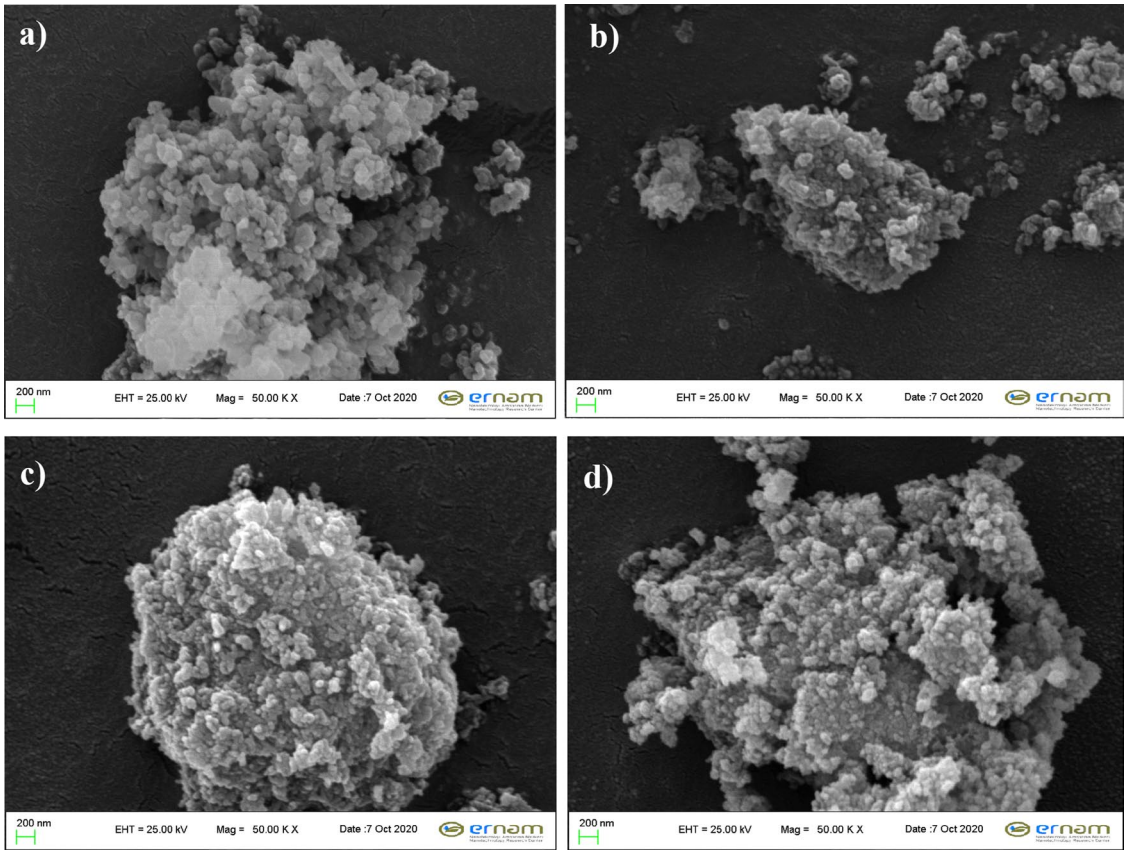

Fig. 1. SEM images of hydrothermally produced and non-heat treated Hydroxyapatite samples, 50000× a) 180°C, 6 hour (HA-6h), b) 180°C, 12 hour (HA-12h) c) 180°C, 18 hour (HA-18h) d)180°C, 24hour (HA-24h)

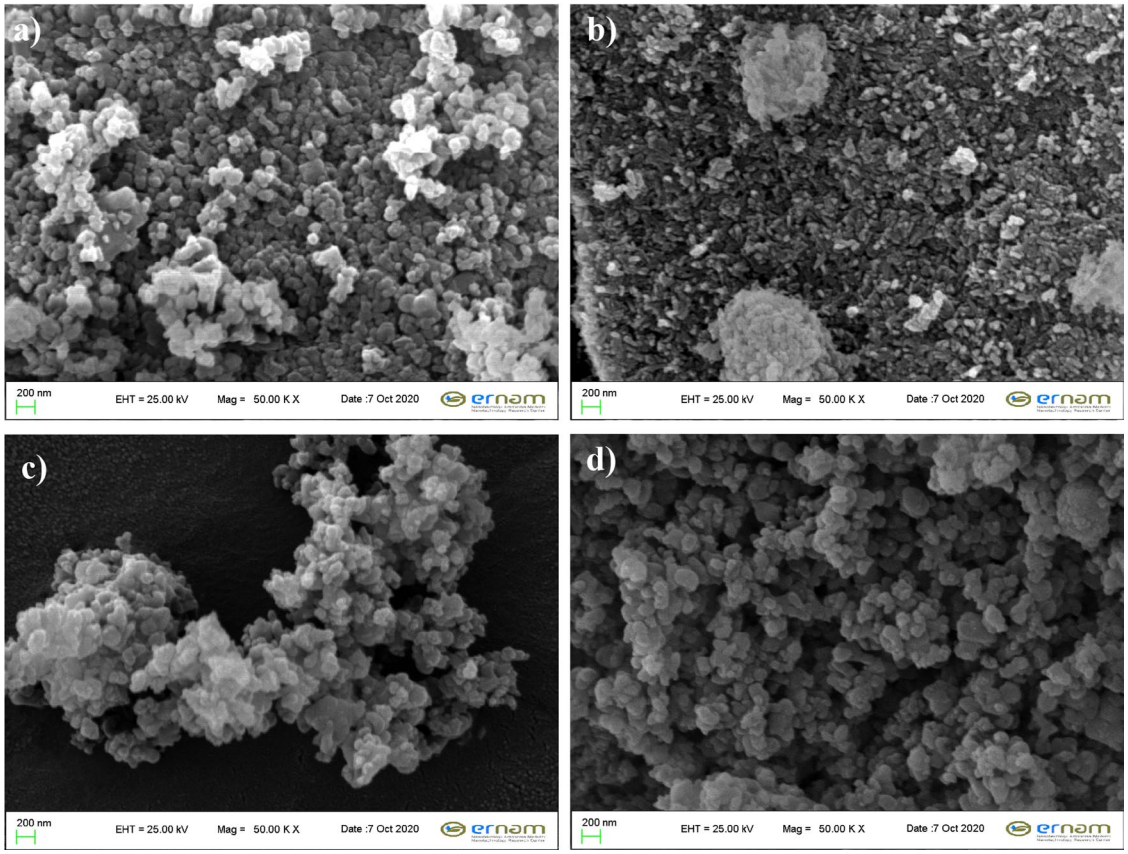

Fig. 2. SEM images of hydrothermally produced and heat treated Hydroxyapatite samples, 50000× a) 180°C, 6 hour (HA-6h-HT), b) 180°C, 12 hour (HA-12h-HT) c) 180°C, 18 hour (HA-18h-HT) d)180°C, 24 hour (HA-24h-HT)

TABLE 2

EDX results of HA-6h, HA-12h and HA-24h-HT samples

Sample	Element/ at.%			
	C	O	Ca	P
HA-6h	60.19	31.13	4.43	4.24
HA-12h	65.91	26.95	3.67	3.46
HA-24h-HT	68.97	26.72	2.32	1.99

3.2. X-Ray Diffraction (XRD) analysis

The X-ray diffraction graph of the samples produced by the hydrothermal method is shown in Fig. 4. The peaks obtained are in compliance with the standard data (JCPDS Card no. – 09-0432) [26]. Within the sensitivity of the X-ray diffraction technique, Hydroxyapatite is the main phase in all samples. It has been observed that the composition and structure of HA are not altered by hydrothermal synthesis. As the hydrothermal reaction time increased, the peaks of the Hydroxyapatites became sharper (HA-18h, HA-24h). Hydrothermal synthesis improved HA crystallinity effectively. However, when the samples produced with the same parameters were heat treatment at 700°C for 1 hour, a decrease was observed in the Hydroxyapatite peaks.

The crystallite sizes of the eight samples synthesized by hydrothermal method were calculated using the Scherrer equation (Eq. (1)) by considering the peak position (002) in the XRD pattern given in Fig. 4. The peak (002) in the XRD graph is a single peak that does not consist of overlapping peaks, and this peak was chosen to calculate the size of the crystal considering reference studies [23].

$$D = \frac{K \times \lambda}{\beta \times \cos\theta} \tag{1}$$

Where,

D – Crystallite size (nm),
K – 0.9 (scherrer's constant),
λ = 0.15406 nm (wavelength of x-Ray source),
β – FWHM (radian),
θ – top position (radian).

The presence of defects in the powders produced by the hydrothermal method was determined by the dislocation density (δ). The dislocation density and micro strain (ε) were calculated by Eq. (2) and Eq. (3) respectively [27].

$$\delta = \frac{\tau}{D^2} \tag{2}$$

$$\varepsilon = \frac{\beta}{4\tan\theta} \tag{3}$$

The crystal sizes (D), dislocation densities (δ) and micro stress (ε) values of the powders calculated with the help of these equations are given in TABLE 3.

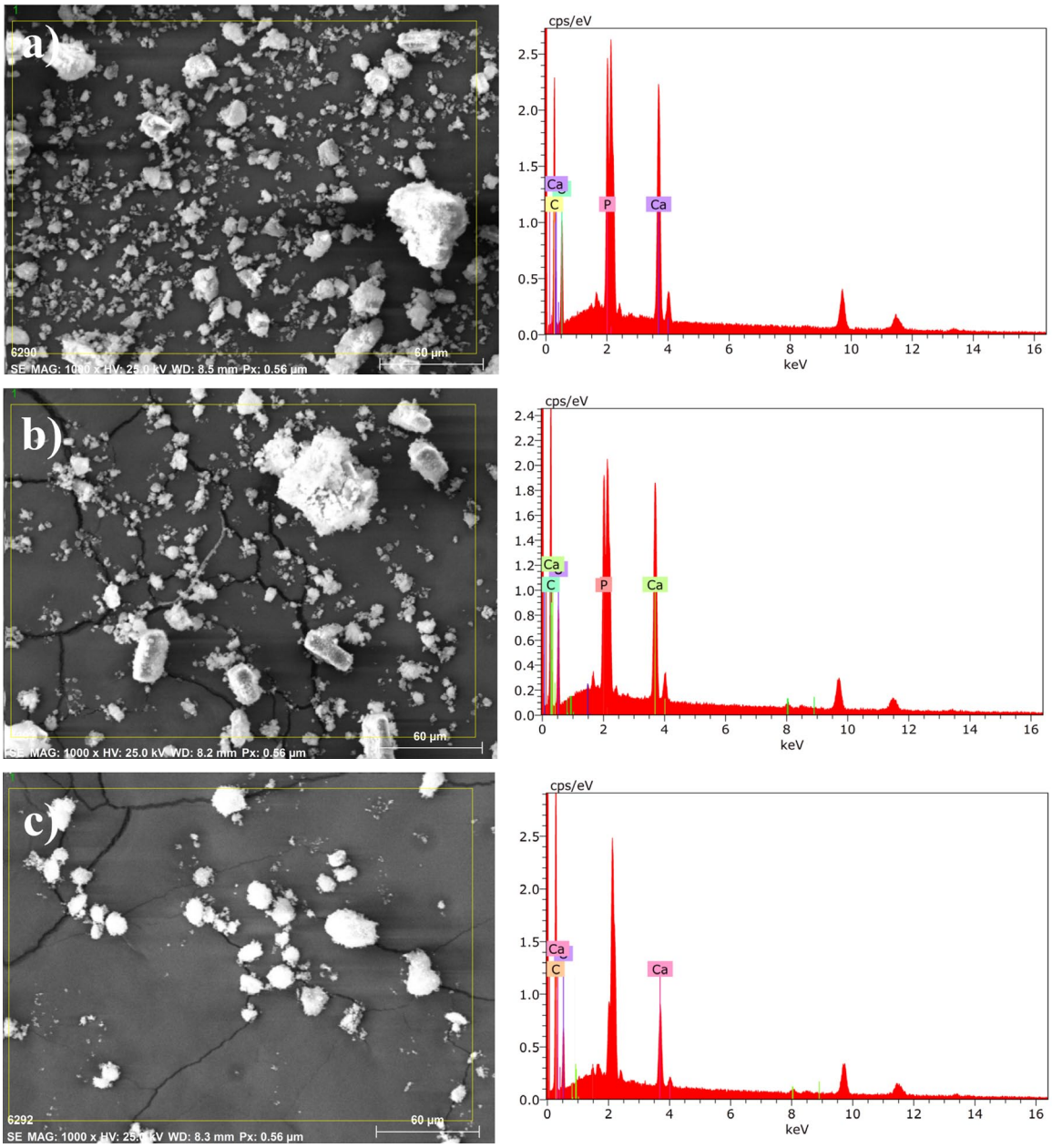

Fig. 3. EDX spectra a) 180°C, 6 hour, non-heat treated (HA-6h) b) 180°C, 12 hour, non-heat treated (HA-12h) c) 180°C, 24 hour, heat treated (HA-24h-HT)

During the hydrothermal synthesis, it was observed that the crystal sizes increased with the increase of sintering time. Especially in HA-18h and HA-24h samples, this increase is observed clearly. When the samples produced with the same parameters were heat treatment, their crystal sizes decreased again.

Sharp peaks in XRD patterns indicate that products crystallize well. A significant difference was observed in the intensity of diffraction peaks between samples due to the different crystallinity. This indicates that the relative density is different between samples and different crystal morphologies are formed. A slight increase in crystallinity was observed in longer hydrothermal reaction times. The increase in crystallinity can be attributed to the restructuring of the clusters in well-organized Hydroxyapatite. The nanoparticles were heat treatment at 700°C for 1 hour to increase crystallinity in dispersed and non-agglomerated

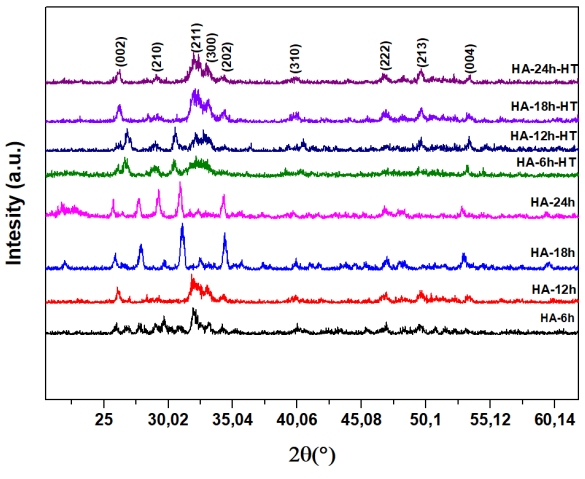

Fig. 4. X-Ray diffraction patterns of Hydroxyapatite samples

TABLE 3

Crystal sizes, dislocation densities and micro stress values obtained using XRD analysis of samples

Sample	D (nm)	$\delta \times 10^{-3}$ (nm)$^{-2}$	$\varepsilon \times 10^{-3}$
HA-6h	13	12.918	11.961
HA-12h	14	13.141	9.510
HA-18h	26	1.508	4.5254
HA-24h	18	15.433	11.484
HA-6h-HT	16	19.344	12.926
HA-12h-HT	17	3.984	7.510
HA-18h-HT	12	26.290	13.233
HA-24h-HT	14	10.027	9.297

Hydroxyapatite microspheres. X-ray diffraction analysis showed that the particles protected their precipitated phases with better crystallinity.

The increased lattice stress resulting from the increase in dislocation density, micro strain, and crystal size is reflected by the increasing broadening of the diffraction peaks with increasing carbonate substitution.

Also, it is very important to adjust the pH value of the solution, otherwise, the pure Hydroxyapatite phase cannot be obtained. As a result of XRD analysis, monetite ($CaHPO_4$ dicalcium phosphate) and the peak corresponding to impurity was not found.

NaOH is an essential reactant in Hydroxyapatite formation. If the dosage of NaOH is not sufficient, excess calcium ions and hydro phosphate ions in the reaction system will react with each other to form calcium hydro phosphate. With increasing dosage of NaOH, the insensitivity of diffraction peaks due to Hydroxyapatite increases, while it decreases due to monetite. When the pH of the Na_2HPO_4 solution is higher than 11.5, characteristic peaks due to monetite are not detected. This reveals that no monetite was produced and pure Hydroxyapatite samples were obtained. NaOH dosage has a great effect on the morphology, composition and crystal structure of the products [28].

3.3. UV-VIS spectroscopy analysis

The UV-Vis spectra of Hydroxyapatite powders produced by hydrothermal synthesis were measured using a laboratory spectrometer in the range of 200-600 nm. Fig. 5a is the absorbance graph of the samples and Fig. 5b is the reflectance graph of the samples. When the absorption graph of Hydroxyapatite powders given in Fig. 5a is examined, since strong absorption can be seen in the UV region, the characteristic wavelength of all samples is around 200-210 nm. It has been observed that the sintering time during the hydrothermal synthesis and the post-synthesis heat treatment greatly affect the absorption rate of the Hydroxyapatite. The absorption rates of the samples increased in direct proportion to the sintering time. The highest absorption occurred in Hydroxyapatite powder (HA-24h) produced at 180°C, 24 hours. When the samples were heat treatment, a significant decrease was observed in the absorption amount of all samples except HA-12h-HT sample. In the reflectance graphics of the Hydroxyapatite powders given in Fig. 5b, it was determined that the sintering time during the hydrothermal synthesis affects the reflectance values. The lowest reflectance ratio was found to be 35-40% at wavelengths of 200-250 nm in HA-24h sample. It was observed around 50% in HA-6h sample, 80% in HA-18h sample and 65% in HA-12h sample. There was an increase in the reflectance rates of the heat treated samples.

Hydroxyapatite is considered to be a material with indirect energy band gap. The bandgap of the samples was calculated with the Tauc plot method using the Tauc relationship (Eq. 4) [23].

$$\alpha h\nu = A\left[h\nu - E_g\right]^n \tag{4}$$

Where,

A – Absorbance,
α – Absorbance constant,
E_g – Band gap,
$h\nu$ – Photon energy,
n – 1/2 (for materials with indirect band gap).

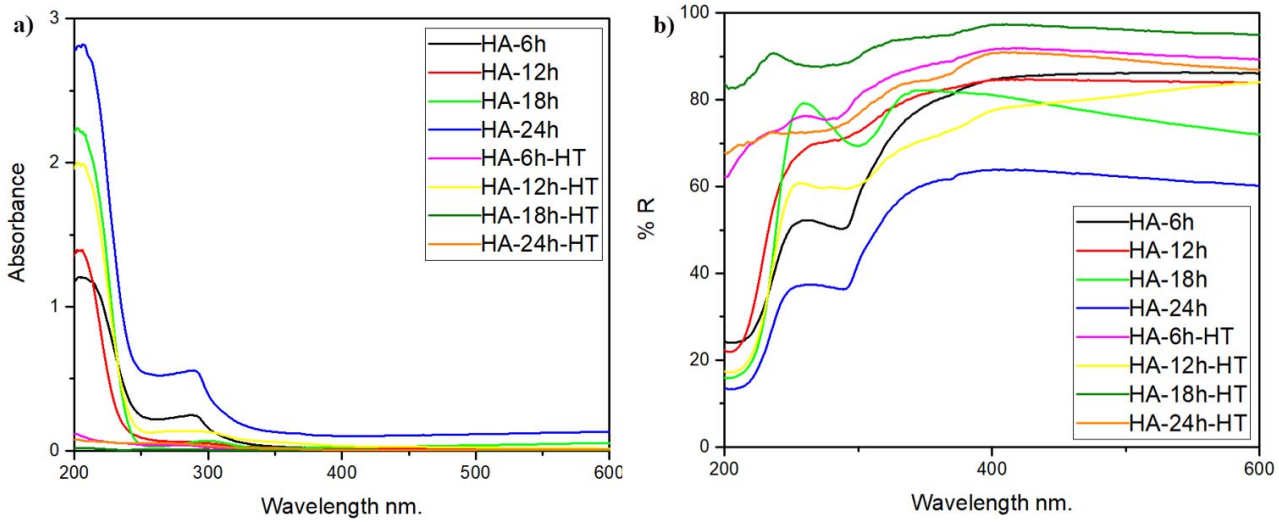

Fig. 5. UV-Vis spectra of Hydroxyapatite samples: a) Absorbance spectra, b) Reflectance spectra

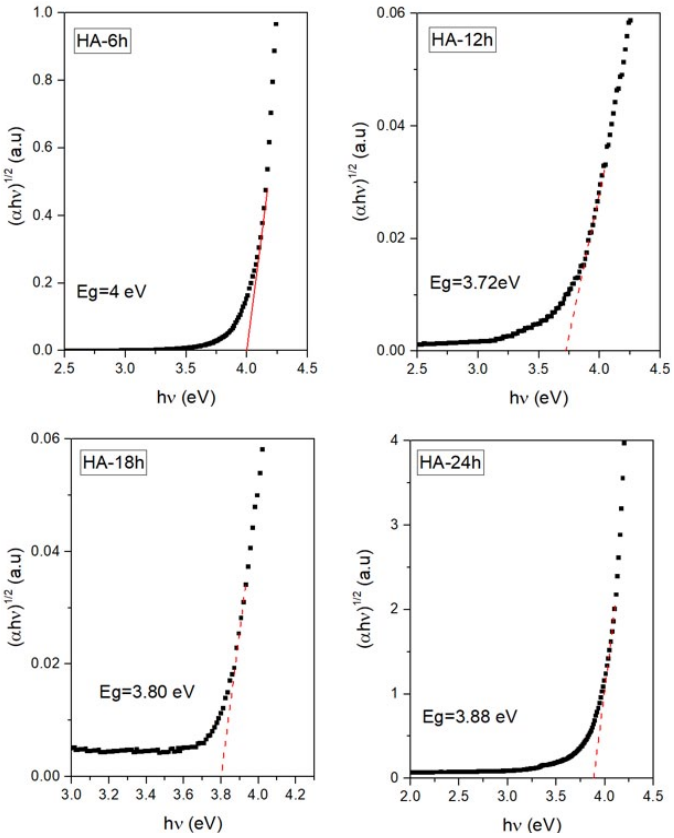

Fig. 6. Energy band gap of non-heat treated Hydroxyapatite samples: a) 180°C, 6 hour (HA-6h), b) 180°C, 12 hour (HA-12h), c) 180°C, 18 hour (HA-18h), d) 180°C, 24 hour (HA-24h)

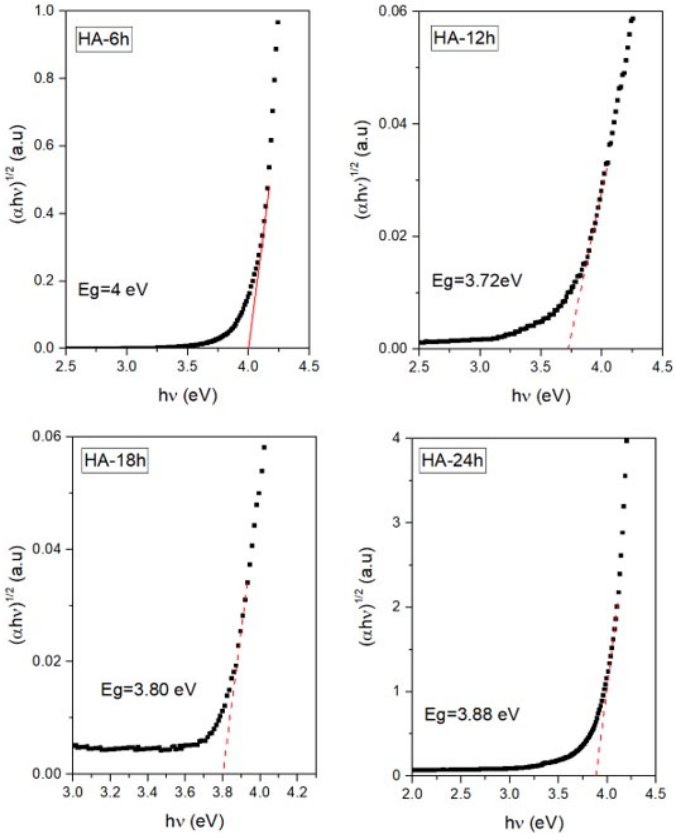

Fig. 7. Energy band gap of heat treated Hydroxyapatite samples: a) 180°C, 6 hour (HA-6h-HT), b) 180°C, 12 hour (HA-12h-HT), c) 180°C, 18 hour (HA-18h-HT), d) 180°C, 24 hour (HA-24h-HT)

Energy band gap of non-heat treated Hydroxyapatite nanopowder for which energy band gap are calculated with Touc Plot Method are given in Fig. 6. Energy band gap of heat treated Hydroxyapatite samples are given in Fig. 7. Eg values of HA-6h, HA-12h, HA-18h and HA-24h samples were found as 4 eV, 3.72 eV, 3.80 eV and 3.88 eV, respectively. Eg values of HA-6h-HT, HA-12h-HT, HA-18h-HT and HA-24h-HT samples were found as 4.05 eV, 3.72 eV, 3.89 eV and 3.96 eV.

4. Conclusions

In this study, pure Hydroxyapatite powders were produced by the Hydrothermal method at high pressure, constant reaction temperature (180°C) and different reaction times (6 hours, 12 hours, 18 hours, 24 hours). The produced powders were divided into two groups and one group was not heat-treatment, and another group was heat-treatment at 700°C for 1 hour. Hydroxyapatite nanopowders were characterized by SEM, EDX, XRD and Uv-Vis. No impurity was observed in the synthesized Hydroxyapatite samples. In Hydroxyapatite powders, it has been observed that the particles are in the form of agglomerates. As the synthesis time increased, more agglomeration occurred. The composition and structure of Hydroxyapatite did not change with the hydrothermal process. As the hydrothermal reaction time increased, the peaks of the Hydroxyapatites became sharper. However, when the samples produced with the same parameters were heat treatment at 700°C for 1 hour, a decrease was observed in Hydroxyapatite peaks. Energy band gap of Hydroxyapatite powders was found between 3.72 eV-4 eV. As the reaction time increased, energy band gap decreased.

Acknowledgments

This study was supported by the Fırat University Scientific Research Projects Unit (Project No: TEKF.18.25).

REFERENCES

[1] C. Zhang, J. Yang, Z. Quan, P. Yang, C. Li, Z. Hou, J. Lin, Hydroxyapatite nano- and microcrystals with multiform morphologies: Controllable synthesis and luminescence properties, Cryst. Growth Des. **9** 2725-2733 (2009).
DOI: https://doi.org/10.1021/cg801353n

[2] M. Sadat-Shojai, M.T. Khorasani, E. Dinpanah-Khoshdargi, A. Jamshidi, Synthesis methods for nanosized hydroxyapatite with diverse structures, Acta Biomater. **9**, 7591-7621 (2013).
DOI: https://doi.org/10.1016/j.actbio.2013.04.012

[3] D.F. Fitriyana, R. Ismail, Y.I. Santosa, S. Nugroho, A.J. Hakim, M. Syahreza Al Mulqi, Hydroxyapatite Synthesis from Clam

Shell Using Hydrothermal Method: A Review, 2019 Int. Biomed. Instrum. Technol. Conf. IBITeC. 7-11 (2019). DOI: https://doi.org/10.1109/IBITeC46597.2019.9091722

[4] R.H. Doremus, Review Bioceramics, J. Mater. Sci. 27 285-297 (1992). https://link.springer.com/content/pdf/10.1007%2FBF00543915.pdf

[5] V.P. Orlovskii, V.S. Komlev, S.M. Barinov, Hydroxyapatite and hydroxyapatite-based ceramics, Inorg. Mater. **38**, 973-984 (2002). DOI: https://doi.org/10.1023/A:1020585800572

[6] M.P. Ferraz, F.J. Monteiro, C.M. Manuel, Hydroxyapatite nanoparticles: A review of preparation methodologies, J. Appl. Biomater. Biomech. **2**, 74-80 (2004).

[7] J. Norton, K.R. Malik, J.A. Darr, I.U. Rehman, Recent developments in processing and surface modification of hydroxyapatite, Adv. Appl. Ceram. (2006). DOI: https://doi.org/10.1179/174367606X102278

[8] S.V. Dorozhkin, Nanosized and nanocrystalline calcium orthophosphates, Acta Biomater. (2010). DOI: https://doi.org/10.1016/j.actbio.2009.10.031

[9] H. Zhou, J. Lee, Nanoscale hydroxyapatite particles for bone tissue engineering, Acta Biomater. (2011). DOI: https://doi.org/10.1016/j.actbio.2011.03.019

[10] D. He, X. Zhang, P. Liu, X. Liu, X. Chen, F. Ma, W. Li, K. Zhang, H. Zhou, Effect of hydrothermal treatment temperature on the hydroxyapatite coatings deposited by electrochemical method, Surf. Coatings Technol. **406**, 126656 (2021). DOI: https://doi.org/10.1016/j.surfcoat.2020.126656

[11] W.J. Shih, Y.F. Chen, M.C. Wang, M.H. Hon, Crystal growth and morphology of the nano-sized hydroxyapatite powders synthesized from CaHPO4·2H2O and CaCO3 by hydrolysis method, J. Cryst. Growth. **270**, 211-218 (2004). DOI: https://doi.org/10.1016/j.jcrysgro.2004.06.023

[12] E.A. Syukkalova, A.V. Sadetskaya, N.D. Demidova, N.P. Bobrysheva, M.G. Osmolowsky, M.A. Voznesenskiy, O.M. Osmolovskaya, The effect of reaction medium and hydrothermal synthesis conditions on morphological parameters and thermal behavior of calcium phosphate nanoparticles, Ceram. Int. **47**, 2809-2821 (2021). DOI: https://doi.org/10.1016/j.ceramint.2020.09.135

[13] S.L. Ortiz, J.H. Avila, M.P. Gutierrez, H. Gomez-Pozos, T.V.K. Karthik, V.R. Lugo, Hydrothermal synthesis and characterization of hydroxyapatite microstructures, 2017 14th Int. Conf. Electr. Eng. Comput. Sci. Autom. Control. CCE 2017. 0-3 (2017). DOI: https://doi.org/10.1109/ICEEE.2017.8108902

[14] X. Jin, J. Zhuang, Z. Zhang, H. Guo, J. Tan, Hydrothermal synthesis of hydroxyapatite nanorods in the presence of sodium citrate and its aqueous colloidal stability evaluation in neutral pH, J. Colloid Interface Sci. **443**, 125-130 (2015). DOI: https://doi.org/10.1016/j.jcis.2014.12.010

[15] Y.P. Guo, Y.B. Yao, C.Q. Ning, Y.J. Guo, L.F. Chu, Fabrication of mesoporous carbonated hydroxyapatite microspheres by hydrothermal method, Mater. Lett. **65**, 2205-2208 (2011). DOI: https://doi.org/10.1016/j.matlet.2011.04.057

[16] S.H. Daryan, J. Javadpour, A. Khavandi, M. Erfan, 1-6. Morphological evolution on the surface of hydrothermally synthesized hydroxyapatite microspheres in the presence of EDTMP, Ceram. Int. **44**, 19743-19750 (2018). DOI: https://doi.org/10.1016/j.ceramint.2018.07.229

[17] N.W. Yan Zhu, Lingling Xu, Chenhui Liu, Caoning Zhang, Nucleation and growth of hydroxyapatite nanocrystals by hydrothermal method, AIP Adv. 8 (2018) 1-11. chrome-extension://dagcmkpagjlhakfdhnbomgmjdpkdklff/enhanced-reader.html?pdf=https%3A%2F%2Fbrxt.mendeley.com%2Fdocument%2Fcontent%2Fc262e4a5-e25d-3d72-83fb-ce56fc85deff (accessed January 21, 2021).

[18] C. García-Negrete, R. Goméz, L. Brun, M. Barrera, G. Arteaga, A. Beltrán, A. Fernández, Synthesis and size evolution of 1D hydroxyapatite crystals under surfactant-free hydrothermal conditions, J. Phys. Conf. Ser. 1386 (2019). DOI: https://doi.org/10.1088/1742-6596/1386/1/012076

[19] W. Kong, K. Zhao, C. Gao, P. Zhu, Synthesis and characterization of carbonated hydroxyapatite with layered structure, Mater. Lett. **255**, 126552 (2019). DOI: https://doi.org/10.1016/j.matlet.2019.126552

[20] W. Liang, Y. Niu, S. Ge, S. Song, J. Su, Z. Luo, Effects of hydrothermal treatment on the properties of nanoapatite crystals, Int. J. Nanomedicine **7**, 5151-5158 (2012). DOI: https://doi.org/10.2147/IJN.S34077

[21] G. Singh, S.S. Jolly, R.P. Singh, Investigation of surfactant role in synthesis of hydroxyapatite nanorods under microwave and hydrothermal conditions, Mater. Today Proc. **26**, 2701-2710 (2019). DOI: https://doi.org/10.1016/j.matpr.2020.02.568

[22] R.P. Singh, G. Singh, H. Singh, Sub-micrometric mesoporous strontium substituted hydroxyapatite particles for sustained delivery of vancomycin drug, J. Aust. Ceram. Soc. **55**, 405-414 (2019). DOI: https://doi.org/10.1007/s41779-018-0248-6

[23] K.J. Joshi, N.M. Shah, Study of Hydroxyapatite Nano-particles synthesized using sono-chemical supported hydrothermal method, Mater. Today Proc. 9-13 (2020). DOI: https://doi.org/10.1016/j.matpr.2020.09.587

[24] R. Zhu, R. Yu, J. Yao, D. Wang, J. Ke, Morphology control of hydroxyapatite through hydrothermal process, J. Alloys Compd. (2008). DOI: https://doi.org/10.1016/j.jallcom.2007.03.081

[25] X. Xiao, R. Liu, F. Liu, X. Zheng, D. Zhu, Effect of poly(sodium 4-styrene-sulfonate) on the crystal growth of hydroxyapatite prepared by hydrothermal method, Mater. Chem. Phys. (2010). DOI: https://doi.org/10.1016/j.matchemphys.2009.12.004

[26] H. El Boujaady, M. Mourabet, A. EL Rhilassi, M. Bennani-Ziatni, R. El Hamri, A. Taitai, Adsorption of a textile dye on synthesized calcium deficient hydroxyapatite (CDHAp): Kinetic and thermodynamic studies, J. Mater. Environ. Sci. **7**, 4049-4063 (2016).

[27] F.Y. Rajhi, I.S. Yahia, H.Y. Zahran, M. Kilany, Synthesis, structural, optical, dielectric properties, gamma radiation attenuation, and antimicrobial activity of V-doped hydroxyapatite nanorods, Mater. Today Commun**. 26**, 101981 (2021). DOI: https://doi.org/10.1016/j.mtcomm.2020.101981

[28] L. An, W. Li, Y. Xu, D. Zeng, Y. Cheng, G. Wang, Controlled additive-free hydrothermal synthesis and characterization of uniform hydroxyapatite nanobelts, Ceram. Int. **42**, 3104-3112 (2016). DOI: https://doi.org/10.1016/j.ceramint.2015.10.099